Journal of Cleaner Production 324 (2021) 129237

Contents lists available at ScienceDirect

Journal of Cleaner Production

journal homepage: www.elsevier.com/locate/jclepro

Utilization of waste sodium sulfate from battery chemical production in neutral electrolytic pickling

Teemu Tuovinen [a,*], Pekka Tynjälä [a,b], Tuomas Vielma [a], Ulla Lassi [a,b]

[a] University of Oulu, Research Unit of Sustainable Chemistry, P.O. Box 3000, FI-90014, Finland
[b] University of Jyvaskyla, Kokkola University Consortium Chydenius, Talonpojankatu 2B, FI-67100, Kokkola, Finland

ARTICLE INFO

Handling Editor: Zhen Leng

Keywords:
Sodium sulfate
Battery chemical
Electrolytic pickling

ABSTRACT

Several industrial activities produce metal sulfates, which are controlled by strict limitations for wastewater concentrations of sulfate. One emerging area where these activities occur is the production of lithium-ion battery chemicals in which sodium sulfates are formed because of cathode precursor co-precipitation. Several solutions for sulfate removal exist, but one option is to reuse the sulfate side stream in other processes to increase circular economy and atom efficiency. In this paper, the reuse of sodium sulfate solution in a steel industry pickling solution is considered. Neutral electrolytic pickling experiments were carried out to compare the pickling behavior of the electrolyte dissolved from pure sodium sulfate and the electrolyte diluted from a side stream solution. Effect of impure electrolyte was evaluated using field emission scanning electron microscopy (FESEM) and energy dispersive X-ray spectrometry (EDS). Concentrations of the metal ions were determined by inductively coupled plasma-optical emission spectrometry (ICP-OES). The results indicated a slight increase in current efficiency with the side stream electrolyte solution, while overall the pickling behavior remained similar. This suggests that a side stream sodium sulfate solution could be used as a pickling electrolyte, reducing the need for pure reagents.

1. Introduction

Both globally and in Finland, several industrial activities (e.g., metal refining, pulp production) produce metal sulfates, which are controlled by strict limitations for wastewater concentrations of sulfate. One emerging area where these activities occur is the production of lithium-ion battery chemicals, especially precursors. For example, in Finland, the limits of the wastewater sulfate concentrations are determined by the environmental permission of the company. The common limit for sulfate concentrations in sewer water is 400 mg L^{-1} (Limits of Water Quality for Sewer Water; Wastewater Limits for Viikinmäen and Suomenojan Water Treatment Plants). Although sulfate ions are not considered hazardous, sulfate limitations are established to reduce the environmental strain caused by the increase in saline concentrations of natural waters, especially in fresh waters. The need to avoid salination while increasing industrial production requires more efficient methods for wastewater treatment, both for sulfate removal and for reusing sulfate-containing solutions. Sulfate recovery methods that reduce the sulfate concentration of purified wastewaters in a commercially viable and efficient way have recently become a point of interest of several studies (Dutrizac and Chen, 2005; Li et al., 2019; Rögener et al., 2012). The promising methods include precipitation of sulfate as sparingly soluble compounds, such as gypsum ($CaSO_4 \cdot 2H_2O$), ettringite ($(Ca_6Al_2(SO_4)_3)(OH)_{12} \cdot 26H_2O$), or barite ($BaSO_4$), with either chemical or electrochemical coagulation, or by separating the sulfate via membranes or ion exchange methods(Ghyselbrecht et al., 2013; Mamelkina et al., 2017; Tun and Groth, 2011). A complementary possibility is to reuse a portion of the side stream sulfate solution in other processes, rather than as a waste, increasing circular economy and atom efficiency.

One possibility that has not been previously explored is the utilization of the sulfate solution from battery precursor production as an electrolyte in the neutral electrochemical pickling of stainless steels. As the final process step at the steel mill, the oxides formed on the surface of the stainless steels during hot rolling and final annealing must be removed by dissolving them together with the chromium-depleted layer that forms underneath the oxides (Li and Celis, 2003). The final dissolution is usually done with a mixed acid solution consisting of nitric and hydrofluoric acids (Li and Celis, 2003; Lindell and Pettersson, 2010; Narváez et al., 2003). However, the reaction produces hazardous nitrous oxides. The emissions can be reduced by limiting the reactants, metals

* Corresponding author.
E-mail address: teemu.tuovinen@oulu.fi (T. Tuovinen).

https://doi.org/10.1016/j.jclepro.2021.129237
Received 25 March 2021; Received in revised form 27 August 2021; Accepted 2 October 2021
Available online 6 October 2021

and metal oxides, entering the system, and immersion time required for scale-free results, including pickling at higher temperatures. Common pre-pickling method is partial electrochemical dissolution of the oxide layer in a near-neutral sulfate solution (pH 2–7) (Braun, 1980; Li and Celis, 2003). This significantly reduces the immersion time required for mixed acid pickling (Hildén et al., 2000, 2001; Ipek et al., 2005a), as the revealed chromium-depleted metallic substrate is rapidly dissolved by a mixture of hydrofluoric acid and nitric acid (Geng et al., 2015; Li and Celis, 2003; Lindell and Pettersson, 2010). The process is known as the Ruthner Neolyte Process or neutral electrolyte pickling (Li and Celis, 2003). Another emerging method for reducing nitrous emissions is to replace the nitric acid with a mimicking mixture of acid(s) and an oxidizing agent, for example, with hydrochloric acid and hydrogen peroxide (Homjabok et al., 2010; Li et al., 2008; Li and Zhao, 2019). As the basics of reactions are similar, neutral electrolytic pickling remains a relevant pre-pickling step.

Originally, Braun suggested that the dissolution was based on reaction between sulfate ions and the oxide layer, activated by electric current (Braun, 1980). The presence of higher valence metallic ions, that is, Cr^{6+}, as chromate ($Cr_2O_7^{2-}$) and Fe^{3+}, in the pickling solution contradicted this mechanism, as their presence is evidence of anodic reactions of the oxides (Shapovalov et al., 1982). The current consensus (Hildén et al., 2000; Li and Celis, 2003; Vynnycky and Ipek, 2009a) seems to be that the neutral electrochemical pickling is based on the anodic dissolution of the oxide scale. The anodic dissolution is especially effective in oxidation of chromium and manganese oxides, the main components of scale after short, low temperature annealing after cold rolling (Airaksinen et al., 2020; Li and Celis, 2003; Zacchetti et al., 2009). A detailed study of the three-step mechanism is given by Hildén et al., 2000, 2001 The related electrochemical reactions are presented in Equations (1)–(5). Equations (1) and (2) describe the bulk reaction for anodic dissolution of chromium oxide at varying pH (Ipek et al., 2005a) described as second step by Hildén et al., 2000, 2001 Equation (3) describes the dissolution of the manganese chromium mixed oxide phase at the beginning of pickling and the first mechanism step described by Hildén et al., 2000, 2001 Manganese is enriched at the early stages of the final annealing (Gonzales et al., 2008). Equations (4) and (5) describe the cathodic and anodic electrolysis of the water, contributed as main reactions in pickling cell as majority of current is spent in them. During pickling, iron oxide is concentrated up to 50 wt% as the surrounding chromium oxide is dissolved. (Hildèn et al., 2000; Schmuki, 1998), The main dissolution reaction becomes inhibited, but after extended polarization at increasing surface over potentials, iron oxide dissolution follows as the third step of the mechanism (Hildén et al., 2000, 2001).

In the mechanism, sodium sulfate appears as an inert electrolyte salt, explaining the relatively low current efficiency of the reaction. Vynnycky and Ipek, 2009a, 2009b also noted the role of sodium sulfate as a secondary electrolyte which conducts current, while developing a mathematical model for neutral electrolytic pickling. Sodium sulfate should be replaceable with different inert salts, without compromising further decrease in pickling efficiency, if the conductivity of the solution is sufficient to reach current densities necessary for scale dissolution (Hildén et al., 2000).

$$Cr_2O_3 + 5H_2O \rightarrow 2CrO_4^{2-} + 10H^+ + 6e^- \quad (1)$$

$$Cr_2O_3 + 4H_2O \rightarrow Cr_2O_7^{2-} + 8H^+ + 6e^- \quad (2)$$

$$MnCr_2O_4 + 8H_2O \rightarrow 2\ HCrO_4^- + MnO_4^- + 14H^+ + 11e^- \quad (3)$$

$$2H_2O\ (l) + 2e^- \rightarrow H_2(g) + 2OH^-(aq) \quad (4)$$

$$2H_2O\ (l) \rightarrow 4H^+(aq) + 4e^- + O_2(g) \quad (5)$$

In an operational electrochemical pickling bath, the electrolyte contains several dissolved metal cations, including Fe^{2+}, Fe^{3+}, Ni^{2+}, Cr^{6+}, Cr^{3+}, in addition to Na^+ and SO_4^{2-} from the pure electrolyte (Shapovalov et al., 1982). The side stream sodium sulfate solution containing nickel ions was tested to be utilized as an electrolyte in neutral electrolytic pickling. Utilization of side stream solution could reduce the need for pure chemicals and the total chemical strain on the environment. As the nickel ions would already be present in pickling bath from dissolution, the required changes in existing water treatment processes should be minimal. Any residual metal ions in the side stream, along with the additional metals dissolved during pickling, should be recoverable during normal wastewater treatment. The improvement of recovery from pickling liquors is already a point of interest in several studies (Dutrizac and Chen, 2005; Rögener et al., 2012; Wieczorek-Ciurowa et al., 2001), and outside the scope of this article.

An industrial neutral electrolytic pickling line runs between sets of driving electrodes. Common materials include steel or stainless steel for cathodes and lead for anodes (Ipek et al., 2005b; Shapovalov et al., 1982). In previous research, Tuovinen et al. (2020) noted that the behavior of directly polarized and bipolar cells differ, and to simulate the industrial process as closely as possible, pickling research should be conducted with a bipolar cell. The bipolar cell has received increased interest recently, and the basics are summarized, for example, by Fosdick et al. (2013) and Crooks (2016)

Experiments were carried out to compare the pickling behavior of an electrolyte dissolved from pure sodium sulfate, referred to as PE, and a solution diluted from a side steam solution, referred to as SE. The comparison was made to determine whether the increased nickel ion concentration or the remaining impurities would affect the pickling results of cold rolled and annealed AISI 304 stainless steel. The effects were evaluated by comparing field emission scanning electron microscopy (FESEM) images with recorded energy-dispersive X-ray spectroscopy (EDS) signals. Concentrations of the metal ions were determined by inductively coupled plasma optical emission spectrometry (ICP-OES). Overall, the aim was to study the suitability of a secondary electrolyte solution for neutral electrolytic pickling using reference samples. If suitable, utilizing side stream would have the potential to decrease the use of primary pure reagent solutions.

2. Experimental

To evaluate the feasibility of side stream solution as a replacement reagent for pure sodium sulfate in the neutral electrolyte pickling efficiency utilizing side stream solution, test solution was acquired from battery production. The tests were carried out in laboratory scale bipolar pickling device, simulating industrial scale line.

2.1. Materials

Side stream sodium sulfate solution was acquired from laboratory-scale precipitation process, producing nickel hydroxide powder as battery chemical precursor material (Välikangas et al., 2020). In previous study, a secondary industrial nickel sulfate side stream containing minor concentrations of iron (Fe, 10.4 mg L^{-1}), cobalt (Co, 14.2 mg L^{-1}), sodium (Na, 18.0 mg L^{-1}) and phosphorous (P, 14.2 mg L^{-1}) as the main impurities was used as the nickel source for the precipitation of $Ni(OH)_2$ using the following method.

Spherical nickel hydroxide ($Ni(OH)_2$) precursor material was synthesized by using hydroxide co-precipitation under an inert atmosphere according to the literature reference (Yang, 2002; Weiwei et al., 2015). The continuously stirred tank reactor precipitation was carried out at a temperature of 40 °C under vigorous mixing. The reactor was preloaded with deionized water, and the aqueous solutions of 1.5 mol L^{-1} $NiSO_4$, 2.5 mol L^{-1} NaOH, and concentrated ammonia were fed to the reactor separately using peristaltic pumps. The feeding rates of the reactants were optimized to achieve a desired precipitation pH level and ammonia concentration in the reactor. At the end of the precipitation process, the solid precursor particles were filtered, washed carefully with deionized water, and dried at 60 °C under vacuum overnight. The leftover filtrate

was collected to be used as the side stream electrolyte (SE) in the pickling research.

Conductivities of the solutions (ion exchanged laboratory water, SE, and PE electrolytes) were determined with a HACH HQ40D-meter (Hach Company, Loveland, CO, USA) connected to a conductivity probe (CDC401; 0–200 mS cm^{-1}). Calibration was tested with 0.1 M KCl solution before measurements. The calculated concentration of sodium sulfate in the filtrate was 0.6 mol L^{-1}, or about 8 wt%. Concentrations of nickel (Ni), iron (Fe), lead (Pb), and chromium (Cr) in the SE were analyzed with the Agilent 5110 VDV ICP-OES (Agilent, Santa Clara, CA, USA). The limits of the error value reported with the results are a combination of the relative standard deviation (*SD*) of the analysis laboratory and error form sample preparation.

As the original precipitation reaction of nickel hydroxide requires a high pH, ca. 12.5, the pH of the side stream sulfate solution was lowered to 3–4 with 2 M sulfuric acid diluted from BAKER ANALYZED Sulfuric Acid, J.T.Baker, 95–98% (MG Scientific, Pleasant Prairie, WI, USA) and diluted to 1:5 with ion-exchanged water prior to pickling to increase the current efficiency of the bipolar cell (Tuovinen et al., 2020). The pH was determined using a HACH HQ40D-meter (Hach Company) connected to a pH probe (PHC10101; pH 2–14). Three-point calibration was carried out using commercial buffers with pH of 4, 7, and 10 (product numbers FF165, FF172, and FF183; FF-Chemicals, Haukipudas, Finland) before measurements. After the dilution, the measured pH and conductivity of the SE solution were 4.0 and 49.1 mS cm^{-1} at room temperature. According Tuovinen et al. (2020), the conductivity matched a 5 wt% sodium sulfate solution of pure grade reagent. During neutralization, the color of the solution changed from blue to clear as the complex between the nickel ions and ammonium decomposed (Grujicic and Pesic, 2006), but no further precipitation was observed.

Ammonium concentration was determined with a HACH HQ40D-meter using an NH4-probe (ISENH4181) from a side stream solution. The solution was diluted with 1 M H_2SO_4 diluted from BAKER ANALYZED Sulfuric Acid, J.T.Baker, 95–98% to reach calibration range of 10–1000 mg L^{-1} (product numbers 15349, 2406549, and 2354153; Hach Company) and to liberate ammonia from the nickel complex. The pH was under 2 after the dilution. The absence of chloride ions was determined from undiluted and filtered side stream solutions by silver chloride precipitation.

The PE sample was used for comparison, and it was prepared from reagent grade sodium sulfate ($Na_2SO_4 \geq 99.0\%$; Honeywell, Seelze, Germany) dissolved in ion-exchanged water (measured conductivity <2 μS cm^{-1}). The final pH of sodium sulfate was adjusted to 4.0 with 2M sulfuric acid. After adjusting the pH, the conductivity of the room temperature PE solution was 48.3 mS cm^{-1}.

The 1.5 mm thick cold-rolled and annealed stainless steel process samples of AISI 304 were obtained from the steel mill at Outokumpu Stainless Oy (Tornio, Finland) and were cut to steel strips of 1.5 cm × 5 cm using a Struers Secotom-10 precision saw (Struers, Ballerup, Denmark) and a 50A20 aluminum oxide cut-off wheel. The nominal elemental composition, as reported by the producer, is provided in Table 1.

2.2. Neutral electrochemical pickling

The neutral electrolyte pickling of the stainless steel was done using the pickling device built at the University of Oulu. The schematics, first described elsewhere (Tuovinen et al., 2020), are shown in Fig. 1. Instead of titanium driving electrodes used previously, two 0.5 mm carbon steel

Table 1
The weight percent (wt%) elemental composition of AISI 304 stainless steel as declared by the producer.

Cr	Ni	Mn_{max}	C	Si_{max}	Fe
18.1	8.1	2	0.04	1	Bal.

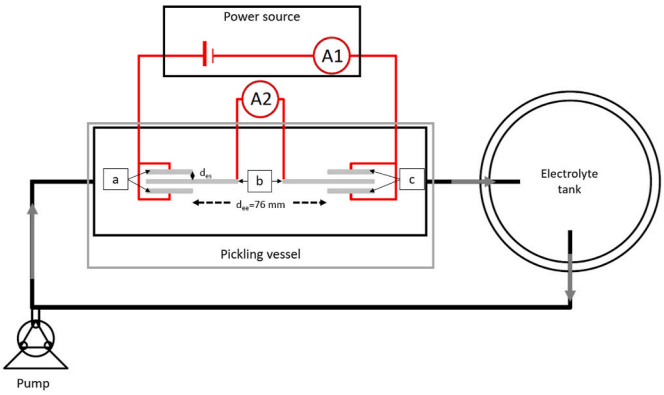

Fig. 1. Measurement system for bipolar pickling. The electrolyte is pumped from the tank to the pickling vessel, and the flow is marked with gray arrows. The vessel is marked with a gray rectangle. From the pickling vessel, the electrolyte flows back to the tank. The power source, marked with a black rectangle, is coupled to the pickling vessel. Amperometers A1 and A2 measure the current inserted into the system and passing sample. Driving electrodes, anodes (a), and cathodes (c), surround samples (b) at a distance of d_{es}, polarizing samples indirectly. The electrode-to-electrode distance (d_{ee}) is 76 mm (Tuovinen et al., 2020).

sheets of 2.5 cm × 2.5 cm were used as driving electrode cathodes, while two 1 cm lead-silver alloys of 3 cm × 2.5 cm were used as driving electrode anodes. The distance between steel strip and driving electrodes was kept at 6 mm. Unlike previously, variation of polarization was not included as lead electrodes would be destabilized during cathodic polarization and manual switching of sample positions could disrupt the sample surfaces by increasing the mechanical strain.

During the pickling, a total of 32 galvanostatic pulses, each 2 s long, were utilized with a 2–4 s pause between pulses for a total pickling time of 2 min and 40 s. The current source recorded (A1) the total current for a total of 2 min and 45 s at a frequency of 200 ms^{-1}, while the amperometer (A2) recorded the sample current at a frequency of approximately 500 ms^{-1}. The current polarized the steel strip closer to steel cathodes anodically, while the steel strip closer to lead anodes was polarized cathodically. The anodic stainless steel strip was regarded as a sample for FESEM-EDS analysis. Cathodic polarization of the samples, simulating the cathodic polarization of steel strips during the industrial pickling process, could not be introduced due to driving electrode materials used in picking. The protective layer in lead anodes stabilized relatively slowly during anodic polarization and would have been destabilized by the localized high alkalinity at the cathodic electrodes, caused by the electrolysis of water described in Equation (4) (Ipek et al., 2007; Shapovalov et al., 1982).

To compare the dissolution rate during pickling, four samples were pickled with a total current of 1 A in both SE and PE electrolytes. The higher current was used to increase current density passing through the samples, and, as noted by Ipek et al. and Hidén et al. (Hildén et al., 2000, 2001; Ipek et al., 2005a), increased the dissolution rate of the oxides.

To compare changes in the electrode surfaces, a pickling experiment was conducted with a total current of 0.6–0.7 A. The pickled samples were analyzed from three positions with FESEM-EDS to observe any changes in the surface of the steel samples. Before the pickling, the measured pH and conductivity of the SE solution were 4.0 and 49.1 mS cm^{-1} at room temperature. The conductivity matched that of a 5 wt% sodium sulfate solution prepared from pure salt (Tuovinen et al., 2020). After preparation of the PE electrolyte, the conductivity and pH were 48.3 mS cm^{-1} and 4.0. The electrolytes were heated to 60 °C prior to pickling. A total of six cold-rolled and annealed AISI304 stainless steel samples were pickled electrochemically with both SE and PE electrolyte solutions. Cathodically polarized samples were not changed between the anodic samples, as the anodic dissolution of the oxide layer remained the

principal mechanism (Hildén et al., 2000, 2001). Cathodic samples were, however, analyzed with FESEM similarly to the anodic samples. In addition, the 500× magnification of the samples was mapped for elements by EDS to compare average changes in element compositions. In addition, the different morphologies were mapped to identify the oxide layer from the metal layer.

3. Results and discussion

3.1. Changes in the electrolytes

Metal concentrations in the solutions were measured using ICP-OES. The results of this analysis are shown in Table 2. Of the analyzed metals, only nickel was found in the undiluted precipitant solution together with a calculated concentration of 8 wt% of sodium sulfate. After the pickling, the relative concentrations of chromium and nickel measured from the PE sample matched those reported by Ipek et al. (2005a) For the SE, the relatively high initial concentration of nickel prevented a similar comparison. The estimated dissolution of nickel, about 0.5 mg L^{-1}, was well within the limit of error of the measurement, 1 mg L^{-1}. In both the PE and SE samples, the iron concentration after the pickling was relatively high, over 20 mg L^{-1}. In a laboratory-scale neutral electrolytic pickling experiment, the dissolved iron concentration remained under 3 mg L^{-1} (Ipek et al., 2005b). As the main mechanism of neutral electrolytic pickling is anodic dissolution of chromium oxide, at least until the very end of pickling (Hildén et al., 2000, 2001; Schmuki, 1998), the analyzed iron concentration suggests that at least some dissolution of the structural steel cathode is happening either during electrolytic pickling or at the down time between samples due to acid dissolution. In addition, some dissolution of the lead anode was observed from the lead concentration in the electrolyte solution, despite the formation of a protective lead oxide layer at the anodes. Dissolution of lead was observed by Shapovalov et al. (1982) and could be attributed to uneven reaction rates that cause changes in solution pH and destabilization of the passive layer of lead anodes.

The ammonium ion concentration determined with HACH was 4.0 g L^{-1} and 0.8 g L^{-1} in diluted solution used in the pickling. No visible precipitation was observed when silver nitrate was added and the mass change of filtered solids was below certainty of scale, 0.1 mg, indicating absence of significant concentrations of chloride ions in the SE solution.

3.2. Changes in the electrodes

To calculate the current efficiency (I_{Eff}) of the cell, the current passing the sample (I_{sample}) was compared to the total current of the cell (I_{total}) as shown in Equation (6).

$$I_{Eff} = \frac{I_{sample}}{I_{total}} \times 100\ \% \tag{6}$$

As the cell was galvanostatic, the cell current was constant during measurement. The sample current was calculated as the average of the recorded values that exceeded 0.2 A to select the peak current from ramp and noise, while the total current exceeding 0.6 A was selected as the peak current. As noted in previous studies (Ipek et al., 2005a; Tuovinen et al., 2020), the calculated current efficiency was higher at higher total currents. The calculated current efficiency was systematically slightly higher, 46% compared with 39%, for the SE than the current efficiency of the PE. The significance of the results passed a *t*-test with confidence interval of 95%. According to Tuovinen et al. (2020), the slightly higher conductivity of the SE solution (49.1 mS cm^{-1} and 48.3 mS cm^{-1}) should lead to a decreased current efficiency of 0.4% when compared with PE efficiency. Therefore, the conductivity differences could not explain the results. The area for the current density calculations of the samples was calculated with half sample length, as the highest current densities concentrate to the half closest to the driving electrodes. The localization of the dissolution in both the SE and the PE samples is exemplified in Fig. 2. Therefore, the current density of the samples was calculated with half length of the samples as an estimation of the area of high current density. The average current density passing sample was 34.4 mA cm^{-2} for the samples pickled in the PE and 39.9 mA cm^{-2} for the samples pickled in the SE.

The FESEM images of the samples pickled in the PE and the samples pickled in SE were seemingly similar, as can be seen in Fig. 3 a and b. The samples remained mostly covered by oxide, but larger areas of chromium depleted layer were revealed, and remaining oxide appeared thinner than in unpickled sample shown in Fig. 3 c. The cathodically polarized samples remained covered by an oxide layer, as can be seen from Fig. 3 d, with small areas of metal substrate visible underneath. This could have been caused by uneven scale formation and scale cracking occurring during cooling, as is common with cold-rolled and annealed austenitic stainless steel samples (Stott and Wei, 1989). EDS analysis of the samples showed only a slight difference in pickling efficiency between samples pickled in the PE and the samples pickled in the SE. Statistically, the most significant difference was the slightly higher nickel concentration at the surfaces of the secondary electrolyte samples. However, the average difference was 0.8% on a minor constituent (nickel concentration of 4.5–7.0 wt% across all measurements, 8.1 wt% as declared by the producer), so it is questionable whether the resolution of the EDS analysis was sufficient for a quantitative estimation of the differences (Newbury and Ritchie, 2013). The other differences were well over a *p*-value of 0.10. The differences remained within uncertainty of the method. Minor concentrations of lead were observed in both cathodes, suggesting some reduction of metals at the cathodic end, although the concentrations remained too low to quantify.

All the anodic samples were manganese free at the areas affected by the highest current density after one pickling cycle with a total current of 0.7 A. When considering the total area of dissolved scale and the initial nickel concentration of the SE, no relevant difference was observed between the composition of SE and PE.

4. Discussion

In the neutral electrolytic pickling mechanism given by Hildén et al., 2000, 2001, the transpassive anodic dissolution of the scale happens in three steps via electrochemical oxidation of metal oxides to higher valence. In the first step, the mixed phase of manganese and chromium oxide is dissolved, as described in Equation (3). Both SE and PE samples reached the second step, where the remaining chromium oxide was dissolved until the remaining iron oxide concentration was increased to 50 wt%, and dissolution was inhibited. It is implied by the given mechanism, and supported by calculations of Vynnycky and Ipek, 2009a, 2009b, that the electrolyte merely acts as an inert conductor between bipolar and driving electrodes, and that the total conductivity should affect the pickling efficiency more than the absolute composition of the electrolyte. These results agree, as the samples were practically identical after pickling in two electrolytes of similar conductivity, but

Table 2
The ICP-OES analysis results for the solutions used in the neutral electrolytic pickling and calculated sodium sulfate concentrations.

Sample	Cr (mg L^{-1})		Fe (mg L^{-1})		Ni (mg L^{-1})		Pb (mg L^{-1})		Na_2SO_4 (wt%)
Ni-precipitation solution	–	–	–	–	175	±5	–	–	8
SE (diluted 1:5 from above) after pickling	0.76	±0.04	24	±1	44	±1	7.5	±0.4	2
PE after pickling	0.63	±0.03	21	±1	0.44	±0.1	8.9	±0.5	5

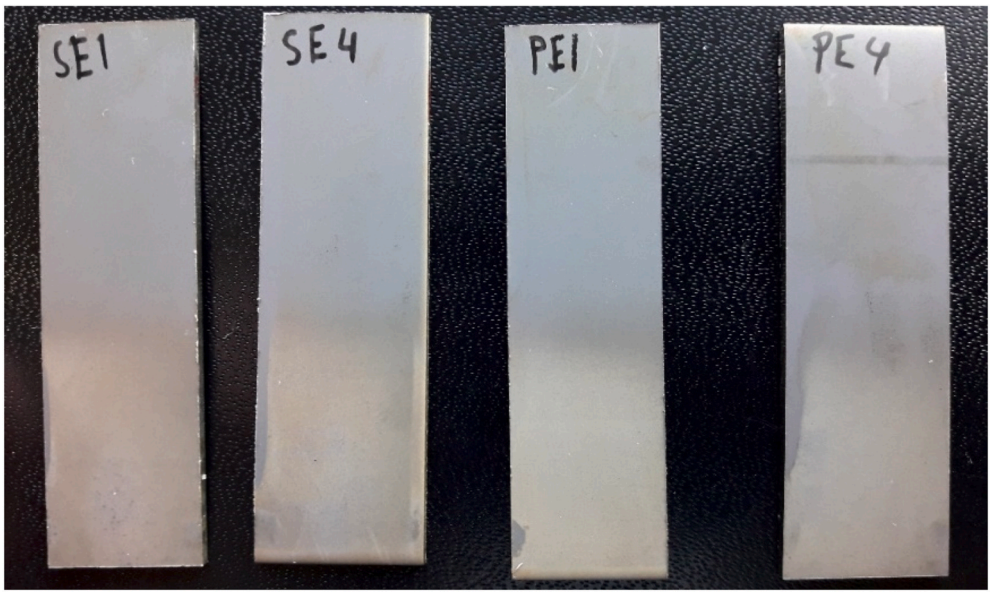

Fig. 2. An example of the localization of the scale dissolution at the sample. Dissolution at the total current of 1A and sample current density of 75 mA cm^{-2}. SE1 and PE1 pickled twice, with total current of 0.6 A and with 0.7 A. SE4 and PE4 pickled with total current of 0.7 A.

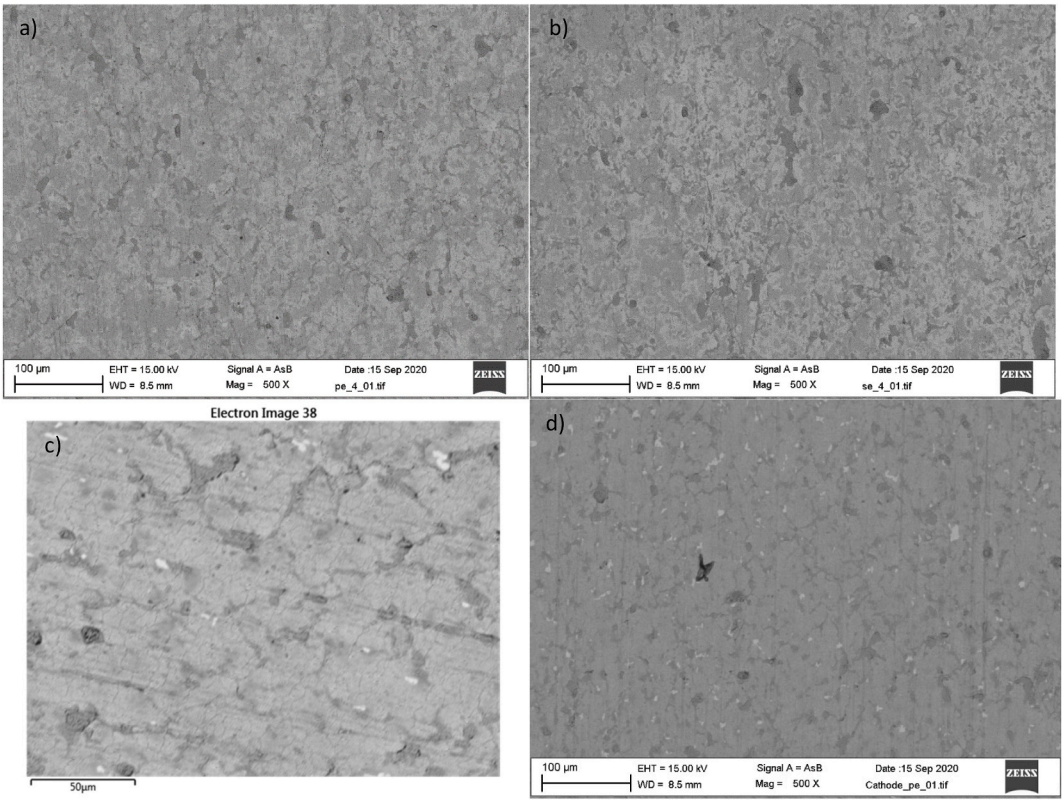

Fig. 3. FESEM images of a) sample pickled in the pure reagent grade sodium sulfate electrolyte, b) pickled in side stream sodium sulfate electrolyte, c) unpickled sample and d) cathodic pure reagent sample. The oxides of pickled samples have thinned, and more chromium depleted layer can be seen between residual scale.

different composition.

When ammonium sulfate was added to the PE solution, no significant drop in pickling efficiency was observed, while the similar addition of sodium sulfate caused the drop in pickling efficiency. The ammonium ion seems to compensate for the drop in efficiency caused by the increased conductivity of the solution. This would explain the observed increase in the pickling efficiency of the side stream electrolyte solution. The increase in the pickling efficiency of the cell is likely caused by the cathodic activity of the ammonium ion, as it can be reduced at the surface of the electrode. However, a high concentration of sodium sulfate was noted to inhibit the reaction. Another possibility is the formation of an iron ammonia complex in the pickling solution. However, neither the effect of iron ion nor the ammonium ion concentration on the current efficiency of bipolar neutral electrolytic pickling has not yet

been reported. Future studies will focus on the effect that the dissolved species have for efficiency of bipolar neutral electrolyte pickling.

Sodium sulfate is an inexpensive and inert electrolyte salt for the neutral electrolyte pickling of stainless steels. The cost of the chemicals required remains rather nominal, and usage of the side stream salt solutions is severely limited by the increased costs of transportation. In addition, the supersaturation of the salt form the solution is possible due to low temperatures during transportation. Typically, a combination of a high concentration of precursor solutions and reaction temperatures are required at precipitation reactions to ensure pure separation of the sparingly soluble products. The clear overflow solution is typically a highly concentrated salt solution. The solubility of sodium sulfate decreases significantly below 32.2 °C, caused by a change in thermodynamically favored phase from sodium sulfate (Na_2SO_4) to metastable sodium sulfate heptahydrate ($Na_2SO_4 \cdot 7H_2O$) and sodium sulfate decahydrate ($Na_2SO_4 \cdot 10H_2O$). The maximum temperature (T °C, when under 32 °C) dependent solubility of sodium sulfate (c_{max}, mol kg^{-1}) can be calculated using Equation (7) (Krumgalz, 2018).

$$c_{max} = 3.241 \times 10^{-1} + 2.838 \times 10^{-2} \times T - 1.48 \times 10^{-3} \times T^2 + 2.57 \times 10^{-4} \times T^3 - 9.122 \times 10^{-6} \times T^4 + 1.438 \times 10^{-7} \times T^5 \quad (7)$$

However, previous research (Tuovinen et al., 2020) suggested that the high concentration of sodium sulfate significantly decreases the efficiency of the bipolar cell used in stainless steel production, as the higher conductivity increased current loss due to driving electrodes short circuiting. An additional step of precipitation of the side product could be introduced while excess heat could be recovered. The lower concentration solution could be beneficial for the system and could increase the temperature range of transportation from 32.2 °C and over to 5 °C and over. For example, after supersaturation at 5 °C, the concentration of sulfate is 6.1 wt%, and after supersaturation at 10 °C, the concentration of sulfate is 8.3 wt%.

The metal concentrations in an industrial neutral electrolytic pickling tank vary from 0.48 to 0.94 g L^{-1} for nickel (II), 0.02–0.57 g L^{-1} for iron (III), 0–0.17 g L^{-1} for iron (II), 0–0.050 g L^{-1} for chromium (VI), and 0.004–0.140 g L^{-1} for chromium (III). When the current is switched off, the iron tends to form iron (III) hydroxide, with concentrations up to 14.6 g L^{-1}. Both chromium (VI) and iron (II) concentrations drop when the current is turned off, suggesting redox reaction between the species (Johnson et al., 1992). The remaining chromate is reduced with sodium sulfite in acidic conditions, the sludge is separated, and the remaining wastewater is mixed with wastewater from mixed acid pickling for neutralization. In mixed acid pickling wastewater, the average nickel concentration can be 10 times higher (Rögener et al., 2012) than residual concentrations measured in this work.

A possible method of wastewater processing is precipitation of the sulfate and reduced chromium (III) as jarosite-type compounds. However, the sensitivity for acid, the relatively high temperature, 230 °C, and a cation that the precipitation reaction requires diminishes its usefulness as a treatment method (Dutrizac and Chen., 2005). In theory, the similar chemistry of chromium (III) and aluminum (III) could be utilized for the ettringite-type precipitation process, but in practice, the reaction requires significant optimization of the reaction conditions to avoid co-precipitation of other metal ions (Wieczorek-Ciurowa et al., 2001). Membrane electrolysis, crystallization, or ion exchange techniques are also studied options for easing the recovery by increasing the concentration of the residual ions in stainless steel production wastewaters (Ghyselbrecht et al., 2013; Tun and Groth, 2011).

The demand for battery materials is predicted to grow significantly in the future, as the number of hybrid and electric cars, energy storage services, and several mobile applications of high energy batteries are all predicted to grow globally in order to reach the goals of carbon emission reductions. The precursor materials for batteries are commonly produced via hydrometallurgical precipitation processes. These processes usually also produce a side stream of a salt solution. Increasing production provides a problem of either finding an alternative usage for this solution or using an efficient desalinization method to avoid strain on the environment. If salt solution remains inert at the process conditions, neutral electrolyte pickling could be one such application, where the side stream solution could be utilized. According to these results, the leftover precipitation solution from nickel hydroxide production could be utilized in such a way. The reaction efficiency was increased, as indicated by the greater extent of the dissolution of the oxide layer when compared with samples pickled in the PE solution.

5. Conclusions

The possibility of using sodium sulfate containing side stream electrolyte (SE) solution from nickel hydroxide production was evaluated as an electrolyte solution in neutral electrolytic pickling of stainless steel. A comparison was made with reagent grade sodium sulfate solution (PE) of comparable conductivity. The main findings were:

- The SE from nickel hydroxide precipitation of battery chemical precursor material production can be used as an electrolyte solution for neutral electrolytic picking of austenitic stainless steel after acidifying the solution with sulfuric acid.
- The current efficiency of the cell is larger when the SE solution is utilized when compared with PE, despite the similar conductivity of the solutions. The increased current efficiency leads to a slight increase in the dissolution of the scale.

CRediT authorship contribution statement

Teemu Tuovinen: Writing – original draft, Investigation, Formal analysis, Methodology. **Pekka Tynjälä:** Resources, Writing – original draft. **Tuomas Vielma:** Supervision. **Ulla Lassi:** Supervision, Conceptualization, Project administration, Funding acquisition.

Declaration of competing interest

The authors declare that they have no known competing financial interests or personal relationships that could have appeared to influence the work reported in this paper.

Acknowledgments

The authors want to acknowledge the research funding by Business Finland (University of Oulu, BATCircle, Dnro 5877/31/2018). We are sincerely grateful to MSc. Elina Riekki of Outokumpu for her advice and support during the research. Ilkka Vesavaara, University of Oulu, is acknowledged for providing ICP-OES results.

References

Airaksinen, S., Tuovinen, T., Laukka, A., Vuolio, T., Heikkinen, E., Riekki, E., Manninen, T., Fabritius, T., 2020. Effect of simulated annealing conditions on scale

formation and neutral electrolytic pickling. Steel Res. Int. 2000449. https://doi.org/10.1002/srin.202000449.
Braun, E., 1980. How to improve pickling of stainless steel strip. Iron Steel Eng. 57, 79–81.
Crooks, R.M., 2016. Principles of bipolar electrochemistry. ChemElectroChem 3, 357–359. https://doi.org/10.1002/celc.201500549.
Dutrizac, J.E., Chen, T.T., 2005. Factors affecting the precipitation of chromium(III) in jarosite-type compounds. Metall. Mater. Trans. B 36, 33–42. https://doi.org/10.1007/s11663-005-0003-6.
Fosdick, S.E., Knust, K.N., Scida, K., Crooks, R.M., 2013. Bipolar electrochemistry. Angew. Chem. Int. Ed. 52, 10438–10456. https://doi.org/10.1002/anie.201300947.
Geng, S., Sun, J., Guo, L., 2015. Effect of sandblasting and subsequent acid pickling and passivation on the microstructure and corrosion behavior of 316L stainless steel. Mater. Des. 88, 1–7. https://doi.org/10.1016/j.matdes.2015.08.113.
Ghyselbrecht, K., Huygebaert, M., Van der Bruggen, B., Ballet, R., Meesschaert, B., Pinoy, L., 2013. Desalination of an industrial saline water with conventional and bipolar membrane electrodialysis. Desalination 318, 9–18. https://doi.org/10.1016/j.desal.2013.03.020.
Gonzales, S., Combarmond, L., Tran, M.T., Wouters, Y., Galerie, A., 2008. Short term oxidation of stainless steels during final annealing. MSF 595–598, 601–610. https://doi.org/10.4028/www.scientific.net/MSF.595-598.601.
Grujicic, D., Pesic, B., 2006. Electrochemical and AFM study of nickel nucleation mechanisms on vitreous carbon from ammonium sulfate solutions. Electrochim. Acta 51, 2678–2690. https://doi.org/10.1016/j.electacta.2005.08.017.
Hildén, J., Virtanen, J., Forsén, O., Aromaa, J., 2001. Electrolytic pickling of stainless steel studied by electrochemical polarisation and DC resistance measurements combined with surface analysis. Electrochim. Acta 46, 3859–3866. https://doi.org/10.1016/S0013-4686(01)00673-9.
Hildén, J.M.K., Virtanen, J.V.A., Ruoppa, R.L.K., 2000. Mechanism of electrolytic pickling of stainless steels in a neutral sodium sulphate solution. Mater. Corros. 51, 728–739. https://doi.org/10.1002/1521-4176(200010)51. :10<728::AID-MACO728>3.0.CO;2-3.
Homjabok, W., Permpoon, S., Lothongkum, G., 2010. Pickling behavior of AISI 304 stainless steel in sulfuric and hydrochloric acid solutions. J. Met. Mater. Miner 20, 1–6. jmmm.material.chula.ac.th/index.php/jmmm/article/view/202.
Ipek, N., Cornell, A., Vynnycky, M., 2007. A mathematical model for the electrochemical pickling of steel. J. Electrochem. Soc. 154, P108. https://doi.org/10.1149/1.2764233.
Ipek, N., Holm, B., Pettersson, R., Runnsjö, G., Karlsson, M., 2005a. Electrolytic pickling of duplex stainless steel. Mater. Corros. 56, 521–532. https://doi.org/10.1002/maco.200403858.
Ipek, N., Lior, N., Eklund, A., 2005b. Improvement of the electrolytic metal pickling process by inter-electrode insulation. Ironmak. Steelmak. 32, 87–96. https://doi.org/10.1179/174328105X23996.
Johnson, C.A., Sigg, L., Lindauer, U., 1992. The chromium cycle in a seasonally anoxic lake. Limnol. Oceanogr. 37, 315–321. https://doi.org/10.4319/lo.1992.37.2.0315.
Krumgalz, B., 2018. Temperature dependence of mineral solubility in water. Part 3. Alkaline and alkaline earth sulfates. J. Phys. Chem. Ref. Data 47, 023101.
Li, H., Zhao, A., 2019. Pickling behavior of duplex stainless steel 2205 in hydrochloric acid solution. Adv. Mater. Sci. Eng. 2019 1–6. https://doi.org/10.1155/2019/9754528.
Li, L.-F., Caenen, P., Celis, J.-P., 2008. Effect of hydrochloric acid on pickling of hot-rolled 304 stainless steel in iron chloride-based electrolytes. Corrosion Sci. 50, 804–810. https://doi.org/10.1016/j.corsci.2007.09.006.
Li, L.-F., Celis, J.-P., 2003. Pickling of austenitic stainless steels (a review). Can. Metall. Q. 42, 365–376. https://doi.org/10.1179/cmq.2003.42.3.365.
Li, X., Lv, M., Yin, W., Zhao, J., Cui, Y., 2019. Desulfurization thermodynamics experiment of stainless steel pickling sludge. J. Iron Steel Res. Int. 26, 519–528. https://doi.org/10.1007/s42243-018-0113-4.
Lindell, D., Pettersson, R., 2010. Pickling of process-oxidised austenitic stainless steels in HNO3-HF mixed acid. Steel Res. Int. 81, 542–551. https://doi.org/10.1002/srin.201000011.
Mamelkina, M.A., Cotillas, S., Lacasa, E., Sáez, C., Tuunila, R., Sillanpää, M., Häkkinen, A., Rodrigo, M.A., 2017. Removal of sulfate from mining waters by electrocoagulation. Separ. Purif. Technol. 182, 87–93. https://doi.org/10.1016/j.seppur.2017.03.044.
Narváez, L., Cano, E., Bastidas, J.M., 2003. Effect of ferric ions in AISI 316L stainless steel pickling using an environmentally-friendly H2SO4-HF-H2O2 mixture. Mater. Corros. 54, 84–87. https://doi.org/10.1002/maco.200390025.
Newbury, D.E., Ritchie, N.W.M., 2013. Is scanning electron microscopy/energy dispersive X-ray spectrometry (SEM/EDS) quantitative?: quantitative SEM/EDS analysis. Scanning 35, 141–168. https://doi.org/10.1002/sca.21041.
Rögener, F., Sartor, M., Bán, A., Buchloh, D., Reichardt, T., 2012. Metal recovery from spent stainless steel pickling solutions. Resour. Conserv. Recycl. 60, 72–77. https://doi.org/10.1016/j.resconrec.2011.11.010.
Schmuki, P., 1998. Electrochemical behavior of Cr_2O_3/Fe_2O_3 artificial passive films studied by in situ XANES. J. Electrochem. Soc. 145, 791. https://doi.org/10.1149/1.1838347.
Shapovalov, E., Shlyamnev, A., Ulyanin, E., Nikitin, V., Fisher, A., Goldzon, D., Popova, L., Milovanov, I., 1982. Investigation of operating parameters of neutral electrochemical pickling bath. Steel USSR 12, 215–219.
Stott, F.H., Wei, F.I., 1989. High temperature oxidation of commercial austenitic stainless steels. Mater. Sci. Technol. 5, 1140–1147. https://doi.org/10.1179/mst.1989.5.11.1140.
Tun, C.M., Groth, A.M., 2011. Sustainable integrated membrane contactor process for water reclamation, sodium sulfate salt and energy recovery from industrial effluent. Desalination 283, 187–192. https://doi.org/10.1016/j.desal.2011.03.054.
Tuovinen, T., Vielma, T., Lassi, U., 2020. Laboratory-scale simulation of industrial neutral electrolytic pickling as a bipolar system—parameters affecting indirect polarization pickling of annealed stainless steel. Eng. Rep. 2, e12245 https://doi.org/10.1002/eng2.12245.
Välikangas, J., Laine, P., Hietaniemi, M., Hu, T., Tynjälä, P., Lassi, U., 2020. Precipitation and calcination of high-capacity LiNiO2 cathode material for lithium-ion batteries. Appl. Sci. 10, 8988. https://doi.org/10.3390/app10248988.
Vynnycky, M., Ipek, N., 2009a. Electrochemical pickling. In: Hegarty, A., Kopteva, N., O'Riordan, E., Stynes, M. (Eds.), BAIL 2008 - Boundary and Interior Layers. Springer Berlin Heidelberg, pp. 287–294.
Vynnycky, M., Ipek, N., 2009b. Supporting electrolyte asymptotics and the electrochemical pickling of steel. Proc. R. Soc. A 465, 3771–3797. https://doi.org/10.1098/rspa.2009.0291.
Weiwei, E., Cheng, J., Yang, C., Mao, Z., 2015. Experimental study by online measurement of the precipitation of nickel hydroxide: effects of operating conditions. Chin. J. Chem. Eng. 23, 860–867. https://doi.org/10.1016/j.cjche.2014.04.004.
Wieczorek-Ciurowa, K., Fela, K., Kozak, A.J., 2001. Chromium(III)-Ettringite formation and its thermal stability. J. Therm. Anal. Calorim. 65, 655–660. https://doi.org/10.1023/A:1017978414203.
Yang, C.-C., 2002. Synthesis and characterization of active materials of Ni(OH)2 powders. Int. J. Hydrogen Energy 27, 1071–1081. https://doi.org/10.1016/S0360-3199(02)00013-7.
Zacchetti, N., Bellini, S., Adrover, A., Giona, M., 2009. Early stage oxidation of AISI 304 stainless steel: role of temperature and oxygen pressure. Mater. A. T. High. Temp. 26, 31–38. https://doi.org/10.3184/096034009X438211.
https://www.oulunvesi.fi/documents/399509/17677332/Viemäriin+johdettavien+jätevesien+raja-arvot/a9cd306e-f126-4f42-b972-d4e27d1bb4da, 2020–. (Accessed 1 February 2021).
https://www.hsy.fi/vesi-ja-viemarit/jateveden-raja-arvot/, 2020–. (Accessed 1 February 2021).